Alternative splicing of the rat sodium/bile acid transporter changes its cellular localization and transport properties

Konstantinos N. Lazaridis*, Pam Tietz*, Ting Wu*, Sertac Kip*, Paul A. Dawson†, and Nicholas F. LaRusso*‡§

*Center for Basic Research in Digestive Diseases, Division of Gastroenterology and Hepatology, Department of Internal Medicine, and ‡Department of Biochemistry and Molecular Biology, Mayo Medical School, Clinic, and Foundation, Rochester, MN 55905; and †Department of Internal Medicine-Gastroenterology, Wake Forest University School of Medicine, Winston-Salem, NC 27157

Communicated by Ralph T. Holman, University of Minnesota, Austin, MN, July 13, 2000 (received for review February 14, 2000)

Bile secretion involves the structural and functional interplay of hepatocytes and cholangiocytes, the cells lining the intrahepatic bile ducts. Hepatocytes actively secrete bile acids into the canalicular space and cholangiocytes then transport bile acids in a vectorial manner across their apical and basolateral plasma membranes. The initial step in the transepithelial transport of bile acids across rat cholangiocytes is apical uptake by a Na^+-dependent bile acid transporter (ASBT). To date, the molecular basis of the obligate efflux mechanism for extrusion of bile acids across the cholangiocyte basolateral membrane remains unknown. We have identified an exon-2 skipped, alternatively spliced form of ASBT, designated t-ASBT, expressed in rat cholangiocytes, ileum, and kidney. Alternative splicing causes a frameshift that produces a 154-aa protein. Antipeptide antibodies detected the ≈19 kDa t-ASBT polypeptide in rat cholangiocytes, ileum, and kidney. The t-ASBT was specifically localized to the basolateral domain of cholangiocytes. Transport studies in *Xenopus* oocytes revealed that t-ASBT can function as a bile acid efflux protein. Thus, alternative splicing changes the cellular targeting of ASBT, alters its functional properties, and provides a mechanism for rat cholangiocytes and other bile acid-transporting epithelia to extrude bile acids. Our work represents an example in which a single gene appears to encode via alternative splicing both uptake and obligate efflux carriers in a bile acid-transporting epithelial cell.

Hepatocytes produce "primary" bile that is delivered to the intestine via the biliary system (1). Primary bile then is modified as it moves through the intrahepatic bile ducts by secretory and absorptive processes of cholangiocytes (2). The "ductal bile" that is formed accounts for ≈40% of total bile in humans (3). Bile acids are polar molecules that require carrier proteins (i.e., transporters) to achieve vectorial transport across plasma membranes. We and others have shown that cholangiocytes absorb bile acids at their apical domain via an apical, sodium-dependent bile acid transporter (ASBT) (4, 5) identical to the 348-aa protein expressed in rat ileum (6) and kidney (7). Because excessive intracellular accumulation of bile acids may lead to cell damage (8), it is imperative that bile acid-transporting epithelia such as cholangiocytes, enterocytes, and renal tubule cells also possess mechanisms to efflux bile acids. Indeed, a previous study supported the existence of a Na^+-independent mechanism for the transport of bile acids at the basolateral domain of biliary epithelia (9). Furthermore, we have reported that normal rat cholangiocytes exhibit apical to basolateral transcellular transport of taurocholate *in vitro* (4). To date, however, the putative transporter that accounts for the extrusion of bile acids at the basolateral domain of cholangiocytes, enterocytes, and renal tubular epithelia has not been identified.

Materials and Methods

Animals. Male Fisher 344 rats (225–250 g) were obtained from Harlan–Sprague–Dawley. *Xenopus laevis* toads (sexually mature female) were purchased from Xenopus I (Ann Arbor, MI). Animals were maintained according to approved protocols by the Mayo Foundation Institutional Animal Care and Use Committee.

Materials. The ZAP Express cDNA synthesis kit was obtained from Stratagene. Oligonucleotide primers were synthesized at the Mayo Molecular Core Facility (Rochester, MN). Reverse transcription and PCR were performed by using the GeneAmp PCR reagent kit and *AmpliTaq* DNA polymerase (Perkin–Elmer). [^{3}H(G)]Taurocholate (specific activity, 3.47 Ci/mmol) of greater than 95% purity by TLC was purchased from DuPont/NEN and [α-^{32}P]UTP (specific activity, 800 Ci/mmol) of greater than 95% purity by TLC was obtained from Amersham Pharmacia. All other reagents were purchased from Sigma unless otherwise indicated.

Construction of Rat Cholangiocyte cDNA Library. Freshly isolated cholangiocytes were purified (>95%) as described (4) from 50 rats previously subjected to bile duct ligation for 2–3 weeks. Total cellular RNA was extracted from cholangiocytes and poly(A)$^+$ mRNA was isolated by using an oligo(dT) column (Stratagene). Subsequently, poly(A)$^+$ mRNA was reversely transcribed and directionally cloned into ZAP Express (Stratagene).

Screening of the Library and Sequencing of Positive Clones. The rat cholangiocyte cDNA library was screened by using a rat ASBT probe (4). Six positive clones were identified after screening ≈1×10^6 plaques. Two of the positive clones were sequenced by using six primers based on the published sequence of rat ASBT (6) (primers BAT1 to BAT6) and two primers specific for the pBK-cytomegalovirus phagemids (primers T3 and T7 from Stratagene). Specifically, BAT1, 5′-TCCTGTCTGTGGCCTCTGGC-3′; BAT2, 5′-CATCGCAGGTGCAATTCTCA-3′; BAT3, 5′-CGTCTTTGCAGCAATAATAT-3′; BAT4, 5′-GACTAGTGATCCATTCTTTT-3′; BAT5, 5′-TATTGTTTAGAAAATGATTG-3′; BAT6, 5′-GAATTCAGAGTTAAATACTT-3′; T3, 5′-AATTAACCCTCACTAAAGGG-3′; and T7, 5′-GTAATACGACTCACTATAGGGC-3′.

Reverse Transcription–PCR (RT-PCR) and Sequence of PCR Products. Total cellular RNA was extracted from scrapings of terminal ileum, whole kidney, and freshly isolated, highly purified cholangiocytes and hepatocytes as described (4). Total cellular RNA

Abbreviations: ASBT, apical Na^+-dependent bile acid transporter; t-ASBT, truncated ASBT; RT-PCR, reverse transcription–PCR; RPA, ribonuclease protection assay.

§To whom reprint requests should be addressed. E-mail: larusso.nicholas@mayo.edu.

The publication costs of this article were defrayed in part by page charge payment. This article must therefore be hereby marked "*advertisement*" in accordance with 18 U.S.C. §1734 solely to indicate this fact.

Article published online before print: *Proc. Natl. Acad. Sci. USA*, 10.1073/pnas.200325297. Article and publication date are at www.pnas.org/cgi/doi/10.1073/pnas.200325297

was further purified with cesium chloride ultracentrifugation, and first-strand cDNA was synthesized by using the SuperScript preamplification system (GIBCO/BRL). Specific oligonucleotide primers that flank the splicing site were synthesized based on the published sequence for rat ASBT (6). Primer F1 was 5′-TTGGAATCATGCCTCTCACAG-3′ (forward) and primer F2 5′-AACAGGAATAACAAGCGCAAC-3′ (reverse). PCR conditions were as follows: 94°C for 2 min; 40 cycles of 94°C for 1 min, 55°C for 1 min, 72°C for 1 min; and 72°C for 10 min. PCR products from each template (i.e., ileum, kidney, and cholangiocytes) were cloned into the pGEM-T Easy Vector, System II (Promega) and sequenced (Mayo Molecular Core Facility).

Quantitative Ribonuclease Protection Assays. The individual pBK-cytomegalovirus phagemids containing rat cDNA clones for either ASBT or truncated ASBT (t-ASBT) were used in separate PCR amplifications to generate specific probes for the full-length or exon-2 skipped ASBT. Each plasmid template was amplified by using the F1 and F2 primers. PCR conditions were as follows: 94°C for 2 min; 40 cycles of 94°C for 1 min, 55°C for 1 min, 72°C for 1 min; and 72°C for 10 min. Each product was isolated and ligated separately into the pGEM-T II Easy Vector. The resulting pGEM-T-II-ASBT and pGEM-T-II-t-ASBT clones were verified by sequencing (Mayo Molecular Core Facility). Antisense ^{32}P-labeled riboprobes were transcribed by using [α-^{32}P]UTP and SP6 polymerase; unlabeled sense strand products were transcribed by using T7 polymerase. Dilutions (0.1, 0.2, 0.5, and 1 ng) of each sense product were used in the ribonuclease protection assay (RPA) to generate standard curves for quantitation of the ASBT and t-ASBT mRNA. Quantitation of RPA was performed by transcribing an unlabelled sense product by using each one of the two clones and T7 polymerase. RPAs were performed by using the RPA II kit (Ambion, Austin, TX) and 30–60 μg of total RNA extracted from different rat tissues and cells as described (4). The radiolabeled antisense RNA transcript from each clone was purified by excision from a 5% acrylamide/8 M urea denaturing gel and subsequently eluted into a solution of 0.5 M ammonium acetate/1 mM EDTA/0.1% SDS at 37°C. Each antisense riboprobe was hybridized with total RNA from the different tissues or isolated cells at 45°C for 12 h. The unhybridized RNA was digested by a mixture of RNase A/T_1 (150–200 units/ml). The protected hybrid (302 bp for ASBT or 183 bp for t-ASBT) was resolved in a 5% acrylamide/8 M urea gel and detected after exposure to x-ray film (Kodak) for 4 h at −70°C. Standard curves for each probe were created by densitometric analysis of the RPA by using the unlabeled sense riboprobe as internal control template (not shown).

Production of Polyclonal Antibodies to t-ASBT and Immunoblotting. The C-13 peptide (Fig. 1) was synthesized and conjugated to keyhole limpet hemocyanin at the Mayo Protein Core Facility. Rabbit polyclonal antibodies were raised to C-13 peptide at Berkeley Antibody (Richmond, CA). Affinity purification of the rabbit antiserum was performed by using the C-13 peptide and an AminoLink Immobilization Kit (Pierce) according to the manufacturer's protocol. Plasma membranes and postnuclear supernatant were loaded on a 12.5% polyacrylamide SDS/PAGE gel. Immunoblots were performed as described (4) by using the affinity purified t-ASBT antibody (1:5,000). Immunodetection was performed by using the enhanced chemiluminescence detection system (Amersham Pharmacia). Specificity of t-ASBT antibody was determined by preabsorption of t-ASBT antibody (1 mg/ml) with the C-13 peptide (2 mg/ml) at 37°C for 1 h.

Immunohistochemistry. Immunohistochemical localization of t-ASBT was performed by using frozen sections (5 μm) of normal rat liver as described (4). The sections were blocked with 5% goat serum and incubated with a 1:50 dilution of t-ASBT antibody at room temperature. Immunodetection was performed by using a goat anti-rabbit IgG biotinylated antibody (1:200 dilution) and the Vectastain ABC kit (Vector Laboratories) from the same vendor.

```
   1  TTAAAAGTTTGGCGTGTTGAAAGTAAGCATTACTCAGCTGGCAATAGAGACAGAACCAGG
  61  GGACTGGTGCTTCTGTGGACTTGGCCATTTGCACAGCACAAGCAGTGATGGATAACTCCT
                                          M  D  N* S  S                5
 121  CCGTCTGTTCCCCAAATGCAACTTTCTGCGAAGGTGATTCCTGCCTAGTAACTGAAAGCA
       V  C  S  P  N* A  T  F  C  E  G  D  S  C  L  V  T  E  S  N     25
 181  ACTTCAATGCCATTCTCAGCACAGTGATGAGCACCGTGCTCACCATTCTTCTAGCCATGG
       F  N  A  I  L  S  T  V  M  S  T  V  L  T  I  L  L  A  M  V     45
 241  TGATGTTTTCTATGGGGTGCAATGTGGAAATCAACAAGTTCCTAGGACACATAAAGCGGC
       M  F  S  M  G  C  N  V  E  I  N  K  F  L  G  H  I  K  R  P     65
 301  CATGGGGCATCTTCGTGGGCTTCCTCTGTCAGTTTGGAATCATGCCTCTCACAGGATTTA
       W  G  I  F  V  G  F  L  C  Q  F  G  I  M  P  L  T  G  F  I     85
 361  TCCTGTCTGTGGCCTCTGGCATCCTTCCTGTGCAGGCTGTGGTGGTGCTAATTATGGGTT
       L  S  V  A  S  G  I  L  P  V  Q  A  V  V  V  L  I  M  G  C    105
 421  GCTGCCCTGGAGGAACTGGCTCCAATATCCTGGCCTATTGGATAGATGGTGACATGGACC
       C  P  G  G  T  G  S  N  I  L  A  Y  W  I  D  G  D  M  D  L    125
 481  TCAGGCATTTCTCTGGTTGCGCTTGTTATTCCTGTTTCCATTGGAATGTTTGTAAATCAC
       R  H  F  S  G  C  A  C  Y  S  C  F  H  W  N  V  C  K  S  Q    145
 541  AAATGGCCCCAAAAAGCGAAGATTATACTTAAAATTGGATCCATCGCAGGTGCAATTCTC
       M  A  P  K  S  E  D  Y  T  •                                   154

 601  ATTGTGCTCATAGCTGTGGTTGGAGGAATACTGTACCAAAGTGCCTGGATCATTGAACCC
 661  AAACTATGGATTATAGGAACAATATTTCCTATAGCTGGCTACAGCCTTGGTTTCTTCCTG
 721  GCTAGACTAGCTGGTCAACCCTGGTACAGGTGCCGAACAGTTGCCTTGGAAACTGGAATG
 781  CAGAACACTCAACTGTGTTCCACCATTGTACAACTCTCCTTTAGCCCTGAGGATCTCAAC
 841  CTTGTGTTCACCTTCCCACTCATCTATACTGTTTTCCAGCTCGTCTTTGCAGCAATAATA
 901  TTAGGAATGTATGTCACATACAAGAAATGTCATGGAAAAAATGATGCTGAGTTTCTAGAG
 961  AAAACAGACAATGATATGGACCCCATGCCATCATTCCAGGAGACAAACAAGGGATTTCAA
1021  CCAGATGAGAAATAGACACTAAGGAGGCAAAAGAAGAAAGCTTCTGGAACAACATTCATT
1081  AAACGAAAACTAAAATTATTTCTTTTGGTGGAATAATCAGCAGAAAAACAAATTTAAAAG
1141  TTAAATTCAAAATTTAAATTATTGGGTTTTTTTGTATAAAGGGACTAGTGATCCATTCTTT
1201  TGTGTGACAAAGGGGTGTGTGTGTGTGTGTGTGTGTGTGTGTGTGTGTGCGCGCGC
1261  GCACGTGCGCGCGCACGTGCATGTGTGTTTACAGGAGTCATTTTTCTGTATCCATGGTCA
1321  GATTGGTCACAAGATATTCCTTGATTCCAAATTCACAGAAGCTTAAGCCTCTTTTATAAA
1381  AAGGCAAAGTGTTTGTATTAATCTCCTATATACTTCAAATCAATATTATCTTACTAAAAT
1441  ATTTAACATGATGTAAATGTTGTGTAAATAGTTGTCCACTGTATTGTTTAGAAAATGATT
1501  GTTTTATGTTTAGTACAGATATCATTTTTCAATATTTTGGCCATAGTTAAAATCATAGAT
1561  GTCAAACATCTTTGGGAGGCCAAAGACATGTACATAGAATGTATAGATAGATAGATAGAT
1621  AGATAGATAGATAGATAGATAGATAGATAGATAGATAGAAGATAGACAGAGAGATA
1681  GCTGATTATCATTAATATATTATCAGAAAACATCTATAGACCTAACTTGATATAGGTCAA
1741  ACTTGAAACTTTGTCATATGTAAGCTGAATTCAGAGTTAAATACTTTGGTATGTAAAAAT
1801  ATAGCATATTACTACTGTAAAATGATTTTTTCTTGAGTGCTTATGATTGTAAGAAGATTG
1861  ATGTGAATGAATTTTAATTATGAATTTTAAATTTTTGCAACATATTTACTTGTGATTTTG
1921  GACTATACTCTGGCAAATGTCTATATTTATATTTTAGAAAAGTAGCTTCAAATGACATTC
1981  TAGAAGTAGAAATGAGAGAAAGCATTACTAATTAATTCAATAACAAATTAGAATTGGATT
2041  AACTTATCTTTTTTTTTATCCATTCGCATACCTCTAGGATCCATTGATACTCATTTTATC
2101  TTTCCAGAAATAGGGCTAATTCAATACAGTTTAAATTTGACAATAATTTTTGGAACTCTG
2161  GAGAGGTTTATTCAAATATGACCTGTATGAAGCAGGTCCAAATGGGCCAATATGATAGCT
2221  ATTCAGCTCATAGGAGGTGCCATACCAGCCACCACGAGCAGGAAGATGTCAGAAGTTACA
2281  AAGGAAAAAAGGTATCAGTCTAGAAAATGACAATGGAGAGACAAATAATACAATGACAAA
2341  TAATACAATGGAGAGACAAAGAAGCATAAA
```

Fig. 1. Nucleotide and deduced amino acid sequences of rat t-ASBT. The nucleotide (top line) and predicted amino acid (bottom line) sequences of the t-ASBT molecule are numbered on the left and on the right of sequences, respectively. The initiator Met and the unique amino acids of t-ASBT after a frameshift of the ORF are in bold (amino acids 126–154). Two potential sites of N-linked glycosylation are marked by *. Putative transmembrane domains are underlined. The C-13 peptide that we synthesized to generate a polyclonal antibody corresponds to the last 13 carboxyl-terminal amino acids of t-ASBT (CKSQMAPKSEDYT).

Expression of ASBT, t-ASBT, and Taurocholate Transport Studies in *Xenopus* Oocytes. Sexually mature female frogs were anesthetized and oocytes were prepared as described (10). After an overnight incubation in modified Barth's solution (10) at 18°C, healthy oocytes were injected with cRNAs, cultured, and exposed to [^{3}H]taurocholate as described (10). During injection experiments, the free intracellular [^{3}H]taurocholate concentration was estimated based on the mass of taurocholate injected (in 50 μl of buffer), the intraoocyte volume (≈500 μl), and the unbound fraction that is free to efflux (≈70%) (11). [^{3}H]Taurocholate efflux from separate oocytes was determined as described (11,

PHYSIOLOGY

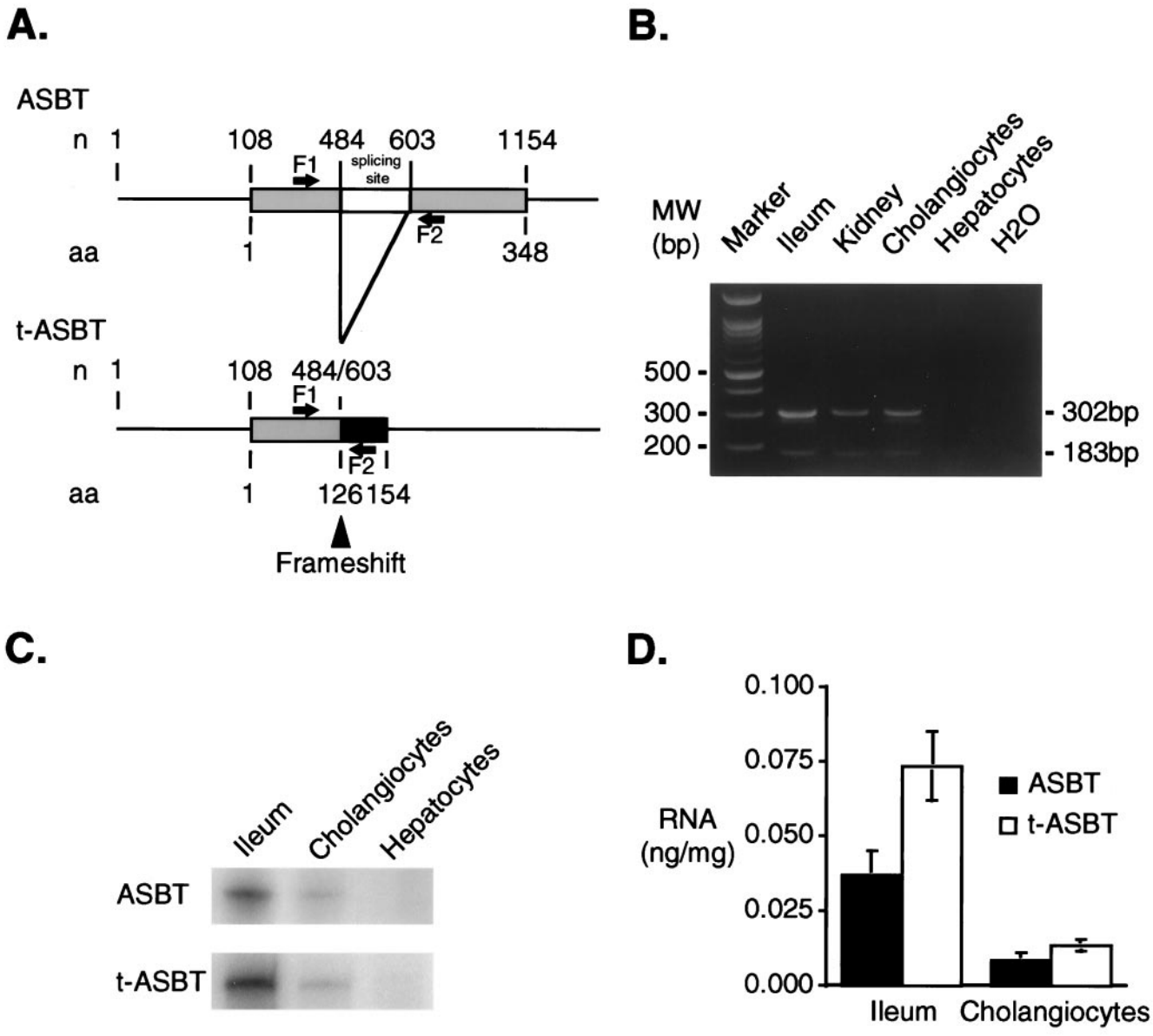

Fig. 2. Molecular analysis of t-ASBT. (*A*) ASBT-splicing sites. Alignment of nucleotide (n) and amino acid (aa) sequences of both ASBT and t-ASBT is shown. The ORF for both molecules starts at nucleotide 108. Alternative splicing occurs between nucleotides 484 and 603 (skipping 119 bp). Exon-2 skipping shifts the reading frame at codon 126 and encodes a predicted 154-aa protein (t-ASBT) with a unique 29-aa carboxyl terminus. Sense (F1: 5′ 334–354 3′) and antisense (F2: 5′ 615–635 3′) primers flanking the splicing site that were used for RT-PCR are shown. (*B*) RT-PCR products corresponding to ASBT and t-ASBT in tissues and cells. Two separate PCR products of 302 bp (ASBT) and 183 bp (t-ASBT) were present in ileum, kidney, and cholangiocytes but not in hepatocytes and the negative control (i.e., H_2O). (*C*) Relative expression of ASBT and t-ASBT message in ileum and cholangiocytes by quantitative RPAs. Representative RPA by using separate specific antisense ^{32}P-labeled riboprobes for ASBT and t-ASBT and SP6 polymerase. Quantitation of RPAs was performed by transcribing an unlabeled sense product for ASBT and t-ASBT by using T7 polymerase. Each sense product (unlabeled riboprobe as internal control template) was used in the RPAs to generate standard curves both for ASBT or t-ASBT (not shown). Both ASBT and t-ASBT transcripts were present in ileum and cholangiocytes but not hepatocytes. (*D*) Densitometric analysis of quantitative RPAs for relative expression of ASBT compared with t-ASBT. Densitometric analysis ($n = 4$) revealed that the t-ASBT mRNA in ileum and cholangiocyte was ≈2 and 1.6 times, respectively, more abundant than the ASBT.

12) by using a Na^+-free incubation medium containing 100 mM choline chloride/2 mM KCl/1 mM $CaCl_2$/1 mM $MgCl_2$/10 mM Hepes-Tris, pH 7.5.

Results

Identification of Rat t-ASBT. In the course of cloning the ASBT from a rat cholangiocyte cDNA library, we identified a unique cDNA clone whose sequence (Fig. 1) encoded a 119-bp deletion corresponding to skipping of exon 2 for the ASBT gene. We designated this cDNA, t-ASBT.

Molecular Analysis of t-ASBT. To determine whether the t-ASBT is expressed in different tissues and cells, RT-PCR was used with oligonucleotide primers that flank exon 2 in the ASBT cDNA (Fig. 2*A*). RT-PCR with RNA from rat ileum, kidney, cholangiocytes, and hepatocytes revealed the presence of 302- and 183-bp products corresponding to the expected transcripts for the ASBT and t-ASBT, respectively (Fig. 2*B*). Subcloning and sequencing verified the identity of the individual products. The relative tissue expression of ASBT and t-ASBT were determined by quantitative RPA by using specific RNA probes and total

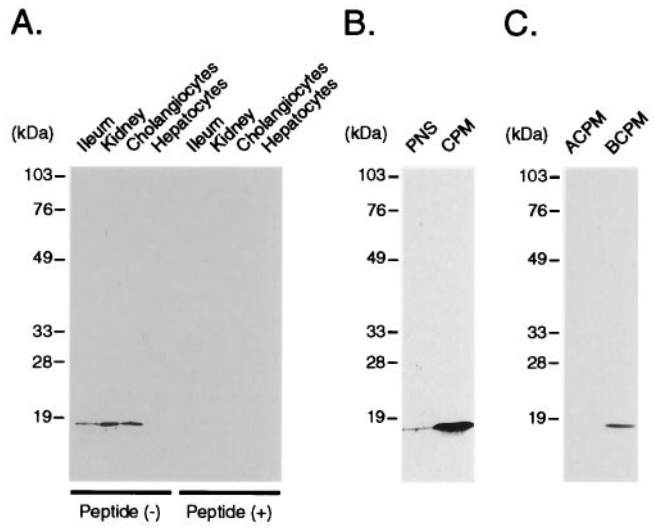

Fig. 3. Immunoblot analysis for t-ASBT in tissues, cells, and cholangiocyte fractions. (*A*) Crude plasma membranes (CPM; 50 μg) from ileum, kidney, cholangiocytes, and hepatocytes were subjected to immunoblotting by using the t-ASBT antibody. An ≈19-kDa band corresponding to t-ASBT was identified in ileum, kidney, and cholangiocytes but not in hepatocytes. Preabsorption of the t-ASBT antibody with C-13 peptide blocked the expression of the t-ASBT-specific band. (*B*) Postnuclear supernatant (PNS; 50 μg) and CPM (50 μg) derived from cholangiocytes were used for immunoblotting with the t-ASBT antibody, which revealed a 30-fold enrichment of t-ASBT protein (≈19 kDa) in CPM compared to PNS. (*C*) Apical cholangiocyte plasma membranes (ACPM; 17 μg) and basolateral cholangiocyte plasma membranes (BCPM) (17 μg) isolated from cholangiocytes were subjected to immunoblotting by using the t-ASBT antibody, which demonstrated the presence of the t-ASBT band exclusively on the BCPM.

cellular RNA from ileum, cholangiocytes, and hepatocytes. As expected, the transcripts for both ASBT and t-ASBT were present in ileum and freshly isolated, highly purified rat cholangiocytes, but not in hepatocytes (Fig. 2*C*). Quantitative densitometric analysis of each message demonstrated that both ASBT and t-ASBT were higher in ileum than in cholangiocytes (Fig. 2*D*). Moreover, the t-ASBT message was ≈2 and 1.6 times greater in ileum and cholangiocytes, respectively, compared with ASBT (Fig. 2*D*).

Expression of t-ASBT Protein. The data summarized in Fig. 2 *C* and *D* suggest that exon-2 skipping is quantitatively important. This alternative splicing produces a frameshift at codon 126 and encodes a predicted 154-aa polypeptide with a unique 29-aa (126–154) carboxyl terminus (Fig. 2*A*). Based on membrane insertion scanning analysis of the human ASBT (13), the t-ASBT polypeptide is predicted to encompass an extracellular amino terminus with two N-linked carbohydrate chains, and three putative transmembrane domains (Fig. 1). To investigate whether the predicted protein product is present in cholangiocytes and other bile acid-transporting epithelia, a synthetic peptide (C-13) corresponding to the C-terminal 13 amino acids (Fig. 1) of the t-ASBT was used to raise polyclonal antibodies. Immunoblot analysis performed by using crude plasma membranes and anti-t-ASBT peptide antibody revealed an ≈19-kDa protein in ileum, kidney, and cholangiocytes, but not in hepatocytes (Fig. 3*A*). Staining of the ≈19-kDa band was abolished by preincubation of the antibody with C-13 peptide (Fig. 3*A*), demonstrating the specificity of the anti-t-ASBT antibody. Consistent with its predicted hydrophobicity, the t-ASBT was enriched ≈30-fold in cholangiocyte crude plasma membranes compared with postnuclear supernatant (Fig. 3*B*). To examine the subcellular localization of the t-ASBT, cholangiocyte crude

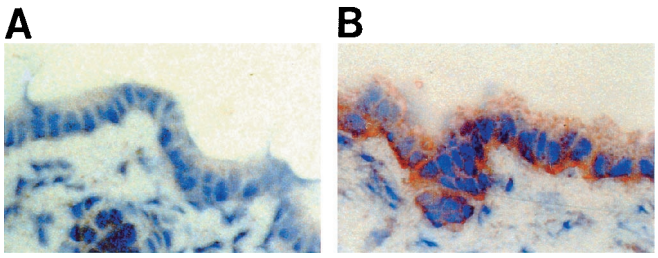

Fig. 4. Indirect immunohistochemistry of t-ASBT in normal rat liver. (*A*) Liver negative control (no primary antibody was used) displays no staining of cholangiocytes (original magnification ×400). (*B*) Liver incubated with primary antibody (anti-t-ASBT; 1:50). The basolateral domain of cholangiocytes is decorated (original magnification ×400).

plasma membranes were fractionated into apical and basolateral domains as described (14). In contrast to the apically expressed ASBT, the alternatively spliced t-ASBT was found exclusively on the basolateral domain (Fig. 3*C*). Although this finding is not directly comparable, it is relevant with previous structure-function studies that localized the apical plasma membrane-sorting signal to the carboxyl-terminal 40 amino acids (308–348) of the full-length ASBT (15).

To localize the t-ASBT protein in whole liver, indirect immunohistochemistry was performed. As can be seen in Fig. 4, the t-ASBT antibody predominately decorates the basolateral domain of cholangiocytes (Fig. 4*B*) in liver, whereas no staining was detected in the negative control (Fig. 4*A*).

Transport Studies in *Xenopus* Oocytes. To determine whether the t-ASBT retains bile acid transport activity, taurocholate uptake was measured as described (10) in *Xenopus* oocytes expressing the t-ASBT. Initially, oocytes were injected with either ASBT RNA (25 ng), t-ASBT RNA (25 ng), or H_2O. Approximately 48 h after injection, the oocytes were incubated with 15 μM [^{3}H]taurocholate for 3 h in the presence or absence of sodium. In agreement with previous studies (6), taurocholate uptake by ASBT RNA-injected oocytes was Na^+-dependent and almost 1,500-fold over the water-injected oocyte background (not shown). No taurocholate uptake was noted in the t-ASBT RNA-injected oocytes over background (not shown). This lack of uptake is consistent with the t-ASBT subcellular expression demonstrated in Fig. 3*C* because the bile acid transport protein(s) residing in the epithelial cell basolateral membrane function(s) primarily in bile acid efflux.

To examine whether the t-ASBT is capable of effluxing bile acids from the cell, *Xenopus* oocytes were injected with ASBT RNA (12.5 ng) alone or mixtures of the ASBT and t-ASBT RNA. The oocytes then were incubated with 15 μM [^{3}H]taurocholate for 3 h in the presence of Na^+ to load the cells. After removing the labeling media and washing with ice-cold stop solution, the intraoocyte [^{3}H]taurocholate accumulation was measured. As expected, oocytes injected with ASBT RNA alone demonstrated significant taurocholate accumulation that was ≈1,400-fold over H_2O-injected cells (Fig. 5*A*). Coinjection of oocytes with ASBT RNA plus increasing concentrations of t-ASBT mRNA resulted in progressively decreased intraoocyte accumulation of taurocholate (Fig. 5*A*). These results are consistent with t-ASBT-mediated efflux, resulting in a lower steady-state accumulation of taurocholate. Because coexpression of the t-ASBT also could have decreased ASBT expression or activity, bile acid efflux experiments also were performed in oocytes by using microinjection as an alternative route for loading the cells with taurocholate.

For these experiments, *Xenopus* oocytes initially were injected with t-ASBT RNA (12.5 ng) or H_2O (control). After incubation

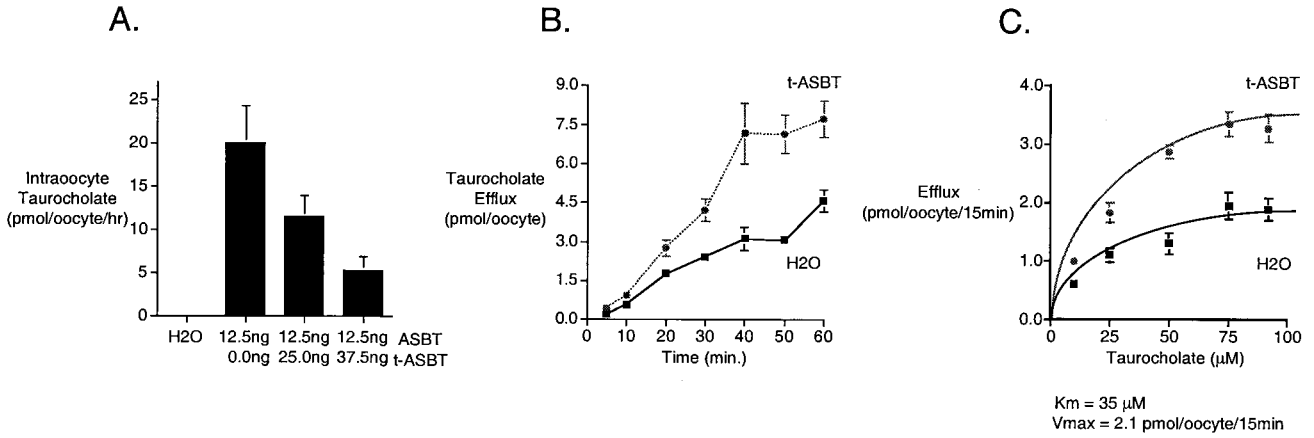

Fig. 5. Transport studies in *Xenopus* oocytes. (*A*) Coinjection of ASBT and t-ASBT in *Xenopus* oocytes. *Xenopus* oocytes were injected with ASBT RNA (12.5 ng) alone or coinjected with the same amount of ASBT and increasing amounts of t-ASBT RNA (25.0 and 37.5 ng). After incubation at 18°C for 48 h, oocytes were exposed to 15 μM [^{3}H]taurocholate for 3 h. After washings with ice-cold stop solution, intraoocyte [^{3}H]taurocholate was measured. ASBT-injected oocytes revealed significant [^{3}H]taurocholate uptake compared with control (i.e., oocytes injected with H_2O). Intraoocyte [^{3}H]taurocholate decreased as the coinjected amount of t-ASBT increased. Data for each bar represent n = 5–7 oocytes. (*B*) [^{3}H]Taurocholate efflux over time in t-ASBT-injected *Xenopus* oocytes. *Xenopus* oocytes were injected with t-ASBT RNA (12.5 ng) or H_2O (control). After incubation at 18°C for 48 h, oocytes were reinjected with [^{3}H]taurocholate to achieve an intraoocyte concentration of 40 μM taurocholate. Data for each ● point represent n = 11–20 oocytes. (*C*) Kinetic parameters of [^{3}H]taurocholate efflux in t-ASBT-injected *Xenopus* oocytes. *Xenopus* oocytes were injected with t-ASBT RNA (12.5 ng) or H_2O (control). After incubation at 18°C for 48 h, oocytes were reinjected with [^{3}H]taurocholate to achieve different intraoocyte concentrations (10–92 μM) of taurocholate. Data for each ● point represent n = 5–7 oocytes.

for 48 h at 18°C, the oocytes were reinjected with [^{3}H]taurocholate to achieve an intraoocyte concentration of 40 μM taurocholate. After washings with ice-cold, sodium-free medium, oocytes were placed in 1 ml of sodium-free efflux medium (24°C), and aliquots (50 μl) were collected over time (5–60 min). As shown in Fig. 5*B*, the t-ASBT-injected oocytes exhibited an increase in taurocholate efflux over time. These values were similar to the activity exhibited in oocytes injected with RNA for the hepatic canalicular bile acid efflux pump (12). The background taurocholate efflux in the H_2O-injected oocytes (Fig. 5*B*) has been attributed to an endogenous *Xenopus* oocytes carrier (11, 12) and was similar to previous studies (12).

To estimate the kinetic parameters of taurocholate efflux, oocytes were injected with t-ASBT RNA (12.5 ng) or H_2O (control) and after 48 h reinjected with [^{3}H]taurocholate to achieve different intraoocyte concentrations (10–92 μM) of taurocholate (11). After washings with ice-cold sodium-free medium, oocytes were placed in 1 ml of sodium-free efflux medium (24°C), and aliquots (200 μl) were collected at 15 min. This time period was chosen because it is within the linear phase of taurocholate efflux in t-ASBT-injected oocytes (Fig. 5*B*). As can be seen in Fig. 5*C*, taurocholate efflux was saturable in oocytes injected with t-ASBT. To estimate the K_m and V_{max} of taurocholate efflux in oocytes injected with t-ASBT, the measured taurocholate efflux in H_2O-injected oocytes (control) (Fig. 5*C*) was subtracted from taurocholate efflux in t-ASBT-injected oocytes at each taurocholate concentration to reflect more accurately the efflux kinetic parameters. Subsequently, by using a kinetic program (ENZFITTER 1.05; Elsevier-Biosoft, Cambridge, U.K.), the apparent K_m and V_{max} were calculated to be 35 μM and 2.1 pmol per oocyte per 15 min, respectively.

Discussion

Our work demonstrates that alternative splicing of the ASBT gene generates an isoform with properties that are complementary to the full-length ASBT. The ASBT functions as a sodium cotransporter to take up bile acids across the apical plasma membrane of bile acid-transporting epithelia (4, 5). In contrast, the t-ASBT is expressed on the basolateral membrane and is predicted to efflux bile acids. This is an example of an epithelial cell transporter where the same gene may encode both the uptake as well as the obligate efflux carrier. Our observation supports the evolving concept that alternative splicing is a biologically important mechanism for generation of related molecules with a novel or complementary function (16). A relevant example is the *apobec-1* gene; almost 50% of the *apobec-1* transcript in adult small intestine and 90% in the developing gut has undergone exon-2 skipping (17). Deletion of *apobec*-1 exon-2 causes a frameshift and encodes a novel 36-aa peptide that is readily detected in enterocytes and colonocytes (18). The mechanism responsible for the exon-2 skipping is not known. It is notable that sequence and gene structure for the ASBT is remarkably similar to the paralogous liver Na^+/bile acid cotransporter (19). The intron/exon junctions fall at homologous amino acid positions for the two genes with the exception that exon 2 of the Na^+/bile acid cotransporter (five exons, total) is further subdivided by an intron at codon 166 in the ASBT gene (six exons, total). This subdivision of exon 2 may have permitted the alternative splicing observed in this study, thereby providing an efflux mechanism for cytotoxic bile acids in ASBT-expressing epithelia. The t-ASBT encodes a 154-aa protein with only three potential membrane-spanning regions. Recent observations from other carriers suggest that small proteins such as the t-ASBT can function in solute transport. For example, selective truncation of the Na^+-glucose cotransporter SGLT1, a protein that normally comprises 13 transmembrane domains, generates a Na^+-independent carrier with properties similar to a facilitative glucose carrier. Indeed, truncated constructs encoding only five or four carboxyl-terminal transmembrane domains of the rabbit or human SGLT1, respectively, were still capable of mediating glucose influx (20).

To date, t-ASBT represents the first identified alternative-spliced molecule that facilitates efflux of bile acids at the basolateral domain of cholangiocytes (and also presumably ileal enterocytes and renal tubular epithelial cells). In the present study, the effect of Na^+, other electrolytes, or ATP on bile acid efflux by t-ASBT was not examined and thus, the driving force for this transporter still needs to be identified. However, there is indirect experimental evidence that a Na^+-independent, carrier-mediated mechanism exists for transport

of conjugated bile acids on the basolateral domain of biliary epithelia (9). Our data suggest that the critical domain(s) for bile acid transport in ASBT lies within the first 125 N-terminal amino acids. We think this proposed function of t-ASBT has physiological relevance. Indeed, efflux of bile acids on the basolateral domain of cholangiocytes by t-ASBT would provide a protective mechanism to prevent deleterious effects of intracellular accumulation of excessive amounts of toxic bile acids in biliary and other bile acid-transporting epithelia expressing the ASBT. Recently, the multidrug resistance protein 3 has been localized to the basolateral membrane of intestinal epithelia and cholangiocytes and transports bile acids in an ATP-dependent manner (21). Considering the toxic effects associated with intracellular bile acid accumulation, it is likely that efflux mechanism(s) for bile acids in cholangiocytes are redundant and that multiple transporters may be involved. Moreover, if t-ASBT has a quantitatively important efflux function in ileal enterocytes, its action also would be crucial to the maintenance of the enterohepatic circulation of bile acids. Whether abnormalities in the expression, cellular localization, or function of t-ASBT result in disease remains to be determined.

We thank Ms. Debbie Hintz for secretarial support. This work was supported by grants from the National Institutes of Health to N.F.L. (DK24031) and P.A.D. (DK47987), by an Advanced Research Training Award to K.N.L. from the American Digestive Health Foundation, and by the Mayo Foundation.

1. Trauner, M., Meier, P. J. & Boyer, J. L. (1998) *N. Engl. J. Med.* **339,** 1217–1227.
2. Roberts, S. K., Ludwig, J. & LaRusso, N. F. (1997) *Gastroenterology* **112,** 269–279.
3. Nathanson, M. H. & Boyer, J. L. (1991) *Hepatology* **14,** 551–566.
4. Lazaridis, K. N., Pham, L., Tietz, P. S., deGroen, P. C., Levine, S., Dawson, P. A. & LaRusso N. F. (1997) *J. Clin. Invest.* **100,** 2714–2721.
5. Alpini, G., Glaser, S. S., Rodgers, R., Phinizy, J. L., Robertson, W. E., Lasater, J., Caligiuri, A., Tretjak, Z. & LeSage, G. D. (1997) *Gastroenterology* **113,** 1734–1740.
6. Shneider, B. L., Dawson, P. A., Christie, D. M., Hardikar, W., Wong, M. & Suchy, F. J. (1995) *J. Clin. Invest.* **95,** 745–754.
7. Christie, D. M., Dawson, P. A., Thevananther, S. & Shneider, B. L. (1996) *Am. J. Physiol.* **271,** G377–G385.
8. Scholmerich, J., Becher, M. S., Schmidt, K., Schubert, R., Kremer, B., Feldhaus, S. & Gerok, W. (1984) *Hepatology* **4,** 661–666.
9. Benedetti, A., Di Sario, A., Marucci, L., Baroni, G. S., Schteingart, C. D., Ton-Nu, H. T. & Hofmann, A. F. (1997) *Am. J. Physiol.* **272,** G1416–G1424.
10. Jacquemin, E., Hagenbuch, B., Wolkoff, A. W., Meier, P. J. & Boyer, J. L. (1995) *Am. J. Physiol.* **268,** G18–G23.
11. Shneider, B. L. & Moyer, M. S. (1993) *J. Biol. Chem.* **268,** 6985–6988.
12. Gerloff, T., Stieger, B., Hagenbuch, B., Madon, J., Landmann, L., Roth, J., Hofmann, A. F. & Meier, P. J. (1998) *J. Biol. Chem.* **273,** 10046–10050.
13. Hallen, S., Branden, M., Dawson, P. A. & Sachs, G. (1999) *Biochemistry* **38,** 11379–11388.
14. Tietz, P. S., Holman, R. T., Miller, L. J. & LaRusso, N. F. (1995) *Biochemistry* **34,** 15436–15443.
15. Sun, A. Q., Ananthanarayanan, M., Soroka, C. J., Thevananther, S., Shneider, B. L. & Suchy, F. J. (1998) *Am. J. Physiol.* **275,** G1045–G1055.
16. McKeown, M. (1992) *Annu. Rev. Cell Biol.* **8,** 133–155.
17. Hirano, K., Min, J., Funahashi, T., Baunoch, D. A. & Davidson, N. O. (1997) *J. Lipid Res.* **38,** 847–859.
18. Lee, R. M., Hirano, K., Anant, S., Baunoch, D. & Davidson, N. O. (1998) *Gastroenterology* **115,** 1096–1103.
19. Oelkers, P., Kirby, L. C., Heubi, J. E. & Dawson, P. A. (1997) *J. Clin. Invest.* **99,** 1880–1887.
20. Panayotova-Heiermann, M., Eskandari, S., Turk, E., Zampighi, G. A. & Wright, E. M. (1997) *J. Biol. Chem.* **272,** 20324–20327.
21. Hirohashi, T., Suzuki, H., Takikawa, H. & Sugiyama, Y. (2000) *J. Biol. Chem.* **275,** 2905–2910.